

# A semi-analytical approach towards efficient ground-track control for Low Earth Orbits

Anna Fontan<sup>(1)</sup>, Klaas Vantournhout<sup>(1)</sup>

<sup>(1)</sup> CS Group GmbH at ESA/ESOC  
Darmstadt, Germany

Email: [anna.fontan@csgroup.de](mailto:anna.fontan@csgroup.de) and [klaas.vantournhout@csgroup.de](mailto:klaas.vantournhout@csgroup.de)

**Abstract – Background:** The Sentinel-1 missions, part of the European Copernicus programme, comprise a pair of satellites in low-Earth orbit (LEO). Their operational constraints adhere to traditional principles, including sun-synchronous frozen orbits with a repeating ground track for periodic study of specific areas of our planet. To maintain payload performance, it is essential to keep the satellite’s ground track close to their reference while maintaining eccentricity near the frozen value. **Purpose:** This study addresses challenges in maintaining the orbital requirements of the Sentinel-1 missions amidst increasing solar activity, which results in unpredictable heightened atmospheric drag, affecting the stability of the orbit. **Method:** This paper proposes an adaptive semi-analytical algorithm to optimise orbit maintenance, providing efficiency and flexible configurability compared to standard propagation algorithms. The algorithm incorporates operator-controlled observables to manage orbit and eccentricity deviations. Manually tuning these observables aids in flexibly handling complex situations, while a standard set of observables would be used for more nominal situations. **Result:** By implementing this semi-analytical algorithm, operators can plan orbit maintenance manoeuvres, minimising violations of operational constraints, and eventually maximising operational efficiency while reducing manual interventions. The approach offers a balance between numerical precision and operational practicality. **Conclusion:** Increasing the orbit maintenance slots and employing a flexible optimisation method are vital to maintain the orbit requirements amidst rising solar activity. The semi-analytical algorithm presents a promising solution to ensure the orbit constraints are satisfied, while minimising operator interventions, ensuring the continuation and quality of crucial Earth observation data.

## I. INTRODUCTION

The Copernicus programme, the Earth Observation component of the European Union Space Programme, aims to provide accurate, easily accessible Earth observation data to enhance environmental management, understand and mitigate the effects of climate change and ensure civil security [1]. The Sentinel missions, ESA’s contribution to the space component of this programme, consists of small constellations of low-Earth orbit (LEO) spacecraft. To meet coverage requirements, the operational orbit constraints adhere to traditional Earth-observation

principles, maintaining repeat-ground track Sun-Synchronous Orbits (SSO) [2], for repeated observations of specific areas of our planet.

Maintaining such orbits presents a challenge due to the stringent mission requirements, ensuring payload performance, and the significant effects of atmospheric drag and Earth’s oblateness. This challenge is particularly pronounced for the Sentinel-1 missions, where the ground track must closely align with its reference while maintaining eccentricity close to its frozen value. In recent years, meeting these constraints has involved performing one manoeuvre sequence per week, for each satellite, in a dedicated orbit maintenance slot.

However, increasing solar activity has made it difficult to maintain the operational constraints of the satellites. Heightened geomagnetic and solar activities combined with solar storms cause greater variability in the outlook and forecast of geophysical and solar data from the National Oceanic and Atmospheric Administration. These data are critical to quantify solar activity, which in turn affects atmospheric density predictions, impacting the atmospheric drag on LEO satellites. Consequently, its variability directly influences the orbit’s predictability as the atmospheric drag affects observables such as ground-track deviation.

To address this issue, increasing the frequency of orbit maintenance slots can assist operators in managing periods of high variability. However, standard propagation algorithms, while offering complete optimisation, often lack the adaptability for operator control and may not be tailored to specific problems. Their configurational complexity, coupled with highly variable solar activity, often necessitates manual reconfigurations to improve the optimisers results. Additionally, extra manoeuvres must sometimes be added. As payload activities take place during the orbit maintenance slots, the extra manoeuvres make avoiding interference with these observation windows more difficult.

While these interventions yield numerically perfect solutions, they are highly time-consuming, highlighting the need for a different optimisation approach. Even though standard propagation algorithms offer complete optimisations by tracking all known time-evaluated disturbances and derivatives, they are especially of interest for tasks where perfect solutions or statistical studies are required. From an operational point of view, the focus is on achieving an optimal solution that meets the requirements, rather than striving for numerical perfection. The purpose of this paper is to define a

sequence of Orbit Control Manoeuvres (OCM) that, when executed, ensure the various operational requirements. This is mainly done by defining a specific set of observables within the operator's control. For the Sentinel-1 missions, these are the ground-track and eccentricity deviations at a designated time. Other missions might have additional orbital requirements such as local-solar time restrictions. Unlike solving the Gauss planetary equations with all known perturbations, the new algorithm takes a single free-drift propagation as input. Since the orbit deviates only slightly from its reference, this free drift approximates known perturbations to a higher order, except for the manoeuvre sequence to be planned. Using this free-drift propagating and the defined observables, all manoeuvres are computed adhering to additional constraints, such as avoiding payload observation windows. The latter is done using standard optimisation algorithms that minimise various cost-functions, quantifying the observables. To avoid costly propagation during the solution search, the algorithm incorporates the manoeuvres and their corresponding effects through a simple linearisation of the Gauss planetary equations.

## II. SUN-SYNCHRONOUS LOW-EARTH REPEAT GROUND TRACK CONTROL STRATEGY

The operational requirements of SSO and LEO missions closely tied to specific observables. For the Sentinel missions, these observables encompass parameters such as the ground track at equator  $\Delta l_0(t)$  and at maximum latitude  $\Delta l_L(t)$ , and the local solar time  $\Delta H(t)$ . These parameters serve as critical indicators of whether the orbital requirements are met.

The observables identified are highly susceptible to external perturbations, including atmospheric drag, third body interactions and higher order gravitational perturbations. The orbital maintenance manoeuvres are needed to counteract the effects of the perturbations on the orbit, by changing the values of the Keplerian elements, i.e. the semi-major axis  $a$ , eccentricity  $e$ , inclination  $i$ , argument of perigee  $\omega$ , and right ascension  $\Omega$ .

While the free-drift secular evolutions in time of  $\Delta l_0(t)$ ,  $\Delta l_L(t)$ , and  $\Delta H(t)$  are assumed known, their rate of change is defined as follows in (1–3) [4].

$$\frac{d^2}{dt^2}(\Delta l_0) \approx -\frac{3}{2}\omega_{TE} \frac{a_e}{a} \frac{da}{dt}, \quad (1)$$

$$\frac{d^2}{dt^2}(\Delta H) \approx -\frac{\omega_{SO}}{\omega_{TE}} \tan i \frac{di}{dt}, \quad (2)$$

$$\frac{d}{dt}(\Delta l_L) \approx \pm a_e \frac{di}{dt}. \quad (3)$$

For LEO, the evolution of  $\Delta l_0(t)$  (1) depends only on the semi-major axis, and results in an eastward long-time parabolic effect drift at the Equator. Analogously,

for SSO if the local time of the satellite is not close to 6h/12h/18h/24h [4], the evolution of  $\Delta H(t)$  is parabolic and depends only on the inclination (2). For  $\Delta l_L$  counted positive towards East, the second term of (3) has positive contribution if the orbit is descending. Eventually, in (1–3)  $\omega_{SO}$  and  $\omega_{TE}$  are the mean velocity of apparent Sun rotation around Earth ( $\omega_{SO} = 2\pi/365.25$  days) and the rotation of Earth ( $\omega_{TE} = 2\pi/1$  day), respectively, and  $a_e$  is the radius of Earth.

The relationships between the observables and the deviation of the Keplerian elements are identified by integrating (1–3). Additional equations link the eccentricity with the observables. For quasi-circular orbits the eccentricity vector  $\vec{e}$  ( $e_x, e_y$ ) can be split in two components as follows [4]:

$$\begin{aligned} e_x &= e \cos \omega, \\ e_y &= e \sin \omega. \end{aligned} \quad (4)$$

However, when considering frozen orbits,  $\omega$  might not be sufficient to determine the position of the satellite on the orbit. Hence, in this analysis the Argument of Latitude (AoL)  $\alpha$  is used instead.

## III. ORBITAL CONTROL MANOEUVRES

The instantaneous increment of  $\Delta a$ ,  $\Delta e$ , and  $\Delta i$  are expressed by the adapted Gauss equations [5]. By tuning the deviations of  $a$ ,  $e$ , and  $i$  with respect to their reference values with OCMs, the desired orbital maintenance control can be achieved (5–8). Indeed, the aim of this section is to explore how manoeuvres can affect the observables. This lays the groundwork for an informed decision-making in orbit maintenance.

$$\Delta a = 2a \frac{\Delta V_T}{V}, \quad (5)$$

$$\Delta e_x = 2 \frac{\Delta V_T}{V} \cos \alpha - \frac{\Delta V_N}{V} \sin \alpha, \quad (6)$$

$$\Delta e_y = 2 \frac{\Delta V_T}{V} \sin \alpha + \frac{\Delta V_N}{V} \cos \alpha, \quad (7)$$

$$\Delta i = \cos \alpha \frac{\Delta V_W}{V}. \quad (8)$$

Here,  $\Delta V$  is the manoeuvre velocity, split in its three components in the orthonormal NTW-reference frame ( $N$  radial,  $T$  tangential, and  $W$  out of plane), and the manoeuvre occurs at  $\alpha(t)$ . Assuming that the manoeuvres happen in optimal conditions, the relationships in (9–11) can be established. To efficiently change  $\Delta i$ , an AoL of 0/180 deg is required; instead, for manoeuvres on  $\Delta a$  and  $\Delta e$ , using the tangential rather than the radial components proves the best results. In (9–11) only the optimal  $\Delta V$  direction for each equation is presented:

$$\Delta a = 2a \frac{\Delta V}{V}, \quad (9)$$

$$\Delta e = 2 \frac{\Delta V}{V}, \quad (10)$$

$$\Delta i = \cos \alpha \frac{\Delta V}{V}. \quad (11)$$

By coupling the integrals of (1–3) and (9–11), the relationships between the observables, the deviation of the Keplerian elements, and the manoeuvres'  $\Delta V$  are defined.

#### A. Orbital control strategy for the ground track at Equator and at maximum latitude

To perform the ground track maintenance at Equator (1) and (9) are used. By integrating (1) twice, and assuming a constant  $da/dt$ , the following equation is derived:

$$\Delta l_0 = -\frac{3}{2} \omega_{TE} \frac{a_e}{a} \Delta a \Delta T = -3 \omega_{TE} a_e \frac{\Delta V}{V} \Delta T, \quad (12)$$

where  $\Delta T = T_{target} - t$  and  $t$  is the mid time of the manoeuvre. Therefore, an increase in semi-major axis leads to a drift towards West. Analogously:

$$\Delta l_L = a_e \frac{\Delta V}{V} \cos \alpha, \quad (13)$$

Therefore, the total contributions to the ground track maintenance given by a series of  $n$ -instantaneous manoeuvres are defined as:

$$\Delta l_0 = -3 \omega_{TE} \frac{a_e}{V} \sum_{i=1}^n \Delta V_i \Delta T_i, \quad (14)$$

$$\Delta l_L = \frac{a_e}{V} \sum_{i=1}^n \Delta V_i \cos \alpha_i. \quad (15)$$

For simplicity, when evaluating the contributions given by a manoeuvre, the changes on the orbital elements due to previous manoeuvres in the same slot are not considered.

#### B. Eccentricity control strategy

The  $\Delta V_i$  needed for eccentricity control can be defined knowing (6), (7) and (10). For a series of  $n$ -instantaneous manoeuvres occurring at time  $t_i$  and AoL  $\alpha_i$ , the resulting eccentricity components are given by (17).

$$\begin{pmatrix} \Delta e_{x,i} \\ \Delta e_{y,i} \end{pmatrix}_0 = 2 \frac{\Delta V_i}{V} \begin{pmatrix} \cos \alpha_i \\ \sin \alpha_i \end{pmatrix}, \quad (16)$$

$$\begin{pmatrix} \Delta e_x \\ \Delta e_y \end{pmatrix} = \sum_{i=1}^n \mathbf{R}(\beta_i) \begin{pmatrix} \Delta e_{x,i} \\ \Delta e_{y,i} \end{pmatrix}_0, \quad (17)$$

where

$$\beta_i = \omega_{ecc}(T_{end} - t_i), \quad (18)$$

$$\mathbf{R}(\beta_i) = \begin{pmatrix} \cos \beta_i & -\sin \beta_i \\ \sin \beta_i & \cos \beta_i \end{pmatrix}. \quad (19)$$

As for  $\Delta l_0$  and  $\Delta l_L$ , also  $\Delta e_x$  and  $\Delta e_y$  depend on the time of the manoeuvre, given  $\alpha_i(t_i)$  and  $\beta_i(t_i)$ . In (17), the evolution in time of the eccentricity vector around its centre of rotation is accounted for through the rotation matrix  $\mathbf{R}(\beta)$ , and the mission-dependent constant  $\omega_{ecc}$  [7].

In (14) the ground track components given by the manoeuvres are evaluated with respect to  $T_{target}$ . The eccentricity contributions, instead, are computed using  $T_{end}$ , which is the time at the end of the slot.

#### C. Local time control strategy

Analogously to the evaluation of  $\Delta l_0(t)$ , by integrating (2) twice and knowing (11) the local time control strategy can be determined, assuming a constant  $di/dt$ :

$$\begin{aligned} \Delta H &= -\frac{\omega_{SO}}{\omega_{TE}} \tan i \sum_{i=1}^n \Delta i_i \Delta T_i \\ &= -\frac{\omega_{SO}}{\omega_{TE}} \tan i \sum_{i=1}^n \frac{\Delta V_i}{V} \Delta T_i \cos \alpha_i. \end{aligned} \quad (20)$$

## IV. OPTIMISATION ALGORITHM

In the preceding section, the groundwork for understanding how manoeuvres impact various observables was established. Building upon this foundation, an optimisation algorithm that determines a sequence of OCMs to meet orbital requirements can now be introduced. The optimisation algorithm follows the standard minimisation approach where the variables of the cost function define the manoeuvres: the execution time  $t_i$  and the manoeuvre size  $\Delta V_i$ . Notably, the number of manoeuvres is not fixed a priori. Instead, the optimiser is iteratively run multiple times with an increasing number of manoeuvres until the termination conditions are met. The goal is to find the minimum number that leads to the best solution. Algorithm 1 outlines the process, with *atol* and *rtol* representing the absolute and relative tolerances, respectively.

---

**Algorithm 1.** Ending Conditions of the Optimisers

---

**for**  $n$  **in** range( $n_{\min}, n_{\max}$ ):  
  evaluate  $\mathcal{J}_n = \min f_{IP}(\vec{\Delta l}_0, \vec{\Delta t})$   
  **if**  $\mathcal{J}_n \leq atol$ : **exit**  
  **if**  $|\mathcal{J}_n - \mathcal{J}_{n-1}| \leq atol$ : **exit**  
  **if**  $\frac{|\mathcal{J}_n - \mathcal{J}_{n-1}|}{\mathcal{J}_n} \leq rtol$ : **exit**

In the context of Sentinel missions, we exploit the possibility of decoupling the observables influenced by out-of-plane (OOP) and in-plane (IP) manoeuvres. Our approach involves a two-step optimisation process. First, we utilize observables obtained from free drift propagation to identify OOP manoeuvres. These OOP manoeuvres inherently introduce higher  $\Delta V$  values and perturbations in observables related to IP manoeuvres. Subsequently, we focus on optimising the IP components using a propagation containing OOP manoeuvres as input. Notably, the alignment-induced in-plane components resulting from OOP manoeuvres are already accounted for during IP optimisation. This decoupling strategy enhances the robustness and accuracy of our solution for Sentinel missions. In the following subsections the cost functions and the input variables of the two algorithms are identified.

#### A. Cost functions of the in-plane optimisation

IP manoeuvres impact the orbit's geometry, specifically the semi-major axis  $a$  and eccentricity  $e$ . Consequently, observables that are affected by these elements, such as eccentricity control and ground-track adjustments at the Equator, shall be considered. Using (14) and (17), we formulate a composite cost function  $\mathcal{J}_n$ , that, when minimised, evaluates to an optimal manoeuvre sequence, meeting the orbital requirements.

The first contributions to the cost function are those that ensure the orbital requirements:

**$\mathcal{J}_{e,max}$ : eccentricity constraint.** This cost function avoids the eccentricity evolution curve to exceed its maximum allowed value  $\Delta e_{max}$ .  $\mathcal{J}_{e,max}$  is the accumulated eccentricity excursion in every ascending node between two consecutive maintenance slots. Hence,  $\mathcal{J}_{e,max}$  drives the eccentricity inside its boundary.

$$\begin{bmatrix} \vec{\Delta e}_{x,m} \\ \vec{\Delta e}_{y,m} \end{bmatrix} = \mathcal{R}(\vec{\beta}_m) \begin{bmatrix} \Delta e_x \\ \Delta e_y \end{bmatrix}, \quad (21)$$

$$\Delta e_j = \sqrt{\Delta e_{x,j}^2 + \Delta e_{y,j}^2}, \quad \text{for } j = 1, \dots, m, \quad (22)$$

$$\mathcal{J}_{e,max} = k_{e,max}^2 \sum_{j=1}^m \max \left( \Delta e_j - \Delta e_{max}, 0 \right)^2, \quad (23)$$

$$\beta_j = \omega_{ecc}(T_j - T_{end}), \quad \text{for } j = 1, \dots, m, \quad (24)$$

where  $\vec{\beta}_m$  is a vector of size  $m$  and represents the rotation angles of the overall eccentricity vector at each  $j^{\text{th}}$ -orbit. Since  $\mathcal{J}_{e,max}$  is a cost function related to the constraint on the eccentricity,  $\mathcal{J}_{e,max}$  is not null only when  $\Delta e_j > \Delta e_{max}$ .

#### **$\mathcal{J}_{\Delta l_0,max}$ : ground track constraints.**

Analogously to  $\mathcal{J}_{e,max}$ , this cost function minimises the time the ground track is over the East ( $\Delta l_{0,East}$ ) or under the West ( $\Delta l_{0,West}$ ) boundaries. The deviations are only evaluated when they exceed the boundaries:

$$\begin{aligned} \mathcal{J}_{\Delta l_0,max} &= k_{\Delta l_0,max}^2 \sum_{j=1}^m \left\{ \max \left( \begin{array}{c} 0 \\ \Delta l_{0,j} - \Delta l_{0,East} \\ \Delta l_{0,West} - \Delta l_{0,j} \end{array} \right) \right\}^2. \end{aligned} \quad (25)$$

Once the orbital requirements are satisfied, supplementary cost functions come into play to address specific objectives. These functions aim to target a desired eccentricity deviation by the end of the maintenance slot and ground track deviations at the beginning of the subsequent slot. Thoughtful selection of these targets is crucial for achieving an optimised trajectory:

**$\mathcal{J}_{\Delta l_0}$ : required  $\Delta l_{0,req}$ .** Given the ground track deviation as function of time  $\Delta l_0(t)$  and the target deviation  $\delta_0$  at time  $T_{target}$ , the total translation that the manoeuvres should compensate for is given by (26). Since (14) is valid for deviations at the Equator, an inclination correction is required (see Fig. 1):

$$\mathcal{J}_{\Delta l_0} = k_{\Delta l_0}^2 \left( \Delta l_{0,req} - \sum_{i=1}^n \Delta l_{0,i} \right)^2, \quad (26)$$

$$\Delta l_{0,req} = \frac{\Delta l_0(T_{target}) - \delta_0}{\sin i}. \quad (27)$$

**$\mathcal{J}_e$ : required  $\Delta e_{req}$ .** Given the eccentricity deviation as function of time and a target eccentricity deviation vector ( $\vec{\Delta e}_{req}$ ) at time  $T_{end}$ , the total eccentricity that the manoeuvres should compensate for is given by (29). The cost function can then be written as:

$$\mathcal{J}_e = \begin{cases} k_e^2 \Delta e_d^2, & \Delta e_d > 0 \\ 0, & \text{otherwise} \end{cases}, \quad (28)$$

$$\Delta e_d = \left\| \vec{\Delta e}_{req} - \sum_{i=1}^n \vec{\Delta e}_i \right\| - r_e. \quad (29)$$

In this context,  $r_e$  is used to either force the eccentricity to reach its target value or to introduce a degree of flexibility (see Fig. 2).

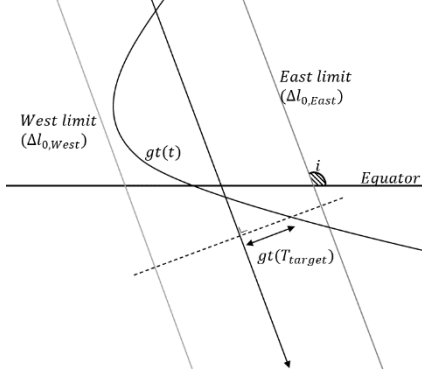


Fig. 1. Ground track evolution at Equator.

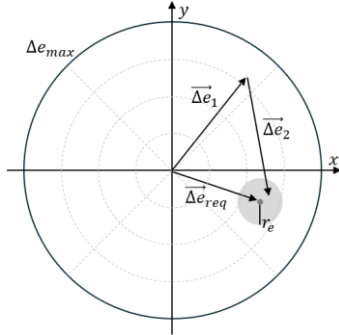


Fig. 2. Eccentricity vector evolution.

In addition to orbital requirements, operational requirements can also be incorporated into the cost function. These typically focus on the timing of the manoeuvres:

**$J_\alpha$ : AoL requirements.** This cost function permits, on a best effort basis, to maintain the AoL within a minimum ( $\alpha_{min}$ ) and a maximum ( $\alpha_{max}$ ) values. Its magnitude is given by the sum of the two contributions:

$$J_\alpha = k_\alpha^2 \sum_{i=1}^n \left\{ \max \left( \begin{array}{c} \alpha_i - \alpha_{max} \\ \alpha_{min} - \alpha_i \end{array} \right) \right\}^2. \quad (30)$$

**$J_{SAR}$ : overlap with payload measurements.** This cost function allows to minimise the overlapping time ( $\Delta\tau$ ) between the manoeuvres and the payload (SAR, Synthetic Aperture Radar) measurements.

$$J_{SAR} = k_{SAR}^2 \sum_{i=1}^n \sum_{j=1}^m \Delta\tau_{i,j}^2, \quad (31)$$

$$\Delta t_i = \frac{\Delta t_{max}}{\Delta v_{max}} \Delta v_i, \quad (32)$$

where  $m$  is the total number of payload intervals measurements in the slot. In the algorithm, the duration of the manoeuvres ( $\Delta t_i$ ) is approximated as in (32) using

the velocity increment.

### B. Cost functions of the out of plane optimisation

In contrast to IP manoeuvres, OOP manoeuvres modify the orbital plane. When placed in an ascending or descending node, they mainly focus on changing the inclination while having little to no effect on the ground track at the Equator. Hence, observables that are influenced by inclination changes, such as the ground track at maximum latitude and the local time control, are considered. Using (15) and (20), we formulate another composite cost function  $J_n$ . Unlike the in-plane (IP) optimisation, where each manoeuvre slot is evaluated individually, the OOP algorithm simultaneously evaluates multiple manoeuvre slots over a period  $\Delta P$ . This different approach stems from the fewer OOP manoeuvres required compared to IP manoeuvres within the same period. Notably, while IP manoeuvres must counteract atmospheric drag, OOP manoeuvres face fewer significant perturbations, resulting in greater predictability of  $\Delta l_L(t)$ .

Cost functions constraining the manoeuvre timing, such as  $J_{SAR}$ , are also used here.

**$J_{\Delta l_L, max}$ : ground track constraints.** This cost function is identical to  $J_{\Delta l_0, max}$  but considers the ground track at maximum latitude instead. As in (25), this cost function is different from zero only when the ground track is outside the constraints ( $\Delta l_{L,j} \leq \Delta l_{L,West}$  or  $\Delta l_{L,j} \geq \Delta l_{L,East}$ ). In (33),  $m$  is the number of orbits in the entire period  $\Delta P$ .

$$J_{\Delta l_L, max} = k_{\Delta l_L, max}^2 \sum_{j=1}^m \left\{ \max \left( \begin{array}{c} 0 \\ \Delta l_{L,j} - \Delta l_{L,East} \\ \Delta l_{L,West} - \Delta l_{L,j} \end{array} \right) \right\}^2. \quad (33)$$

**$J_{\Delta H}$ : local time constraints.** The definition of  $J_{\Delta H}$  is similar to the cost functions constraining the ground-track  $J_{\Delta l_0, max}$  and  $J_{\Delta l_L, max}$  defined in (25) and (33). The curve of the local time  $\Delta H(t)$  is constrained by an upper ( $\Delta H_{max}$ ) and lower ( $\Delta H_{min}$ ) boundaries; only the points of  $\Delta H(t)$  that exceed these values are considered.

**$J_{\Delta V}$ : minimise total  $\Delta V$ .** With this cost function the minimum  $\Delta V$  is achieved. Since  $\Delta l_L(t)$ , unlike  $\Delta l_0(t)$ , does not have a final value to achieve at a certain  $T_{target}$ , its evolution in time can have different solutions for different  $\Delta V$ .  $J_{\Delta V}$  (34) is used to achieve the most efficient one.

$$J_{\Delta V} = k_{\Delta V}^2 \sum_{i=1}^n \Delta V_i^2. \quad (34)$$

**$J_{\Delta t}$ : time between the final point and the mid times of the manoeuvres.**

The following cost function allows to delay as much as possible the OOP manoeuvres in the  $\Delta P$  period. It allows to avoid planning manoeuvres in the upcoming slot that would be discarded once the future curve evolution is known.

$$J_{\Delta t} = k_{\Delta t}^2 \sum_{i=1}^n (T_{end} - t_i)^2, \quad (35)$$

where  $T_{end}$  is the final time of  $\Delta P$ .

## V. NUMERIC RESULTS

### A. Sentinel-1A mission requirements.

Sentinel-1A is in a low-Earth, Sun-synchronous, frozen eccentricity orbit with a mean solar local time at the ascending node (MSLTAN) equal to 18:00 UTC. It follows a reference orbit with a 12 days repeat cycle, which orbital elements are  $a \approx 7080.1$  km,  $i \approx 98.2$  deg, and  $V \approx 7.5$  km/s, and  $\omega_{ecc} \approx -115.56$  days $^{-1}$ . To maintain the ground track within the constraints, equal to  $\Delta l_{max} = \pm 120$  m with respect to the reference orbit at Equator and at maximum latitude, as of January 2024 two batches of manoeuvres are used per week. These slots are on Tuesday-Wednesday and Friday-Saturday from 21:15 UTC to 01:45 UTC. The  $\Delta e$  has to be kept below  $\Delta e_{max} = 8.4 \times 10^{-6}$  to satisfy the altitude requirement (60 meters of radial deviation), and the MSLTAN shall be within  $\Delta H_{max/min} = \pm 5$  mins with respect to the reference value. The value of  $\delta_0$  is set equal to 15 and 12 meters when the manoeuvres are performed on the Tuesday and Friday slots, respectively. The value of  $\Delta e_{req}$  instead varies during the year [7].

To avoid reaction wheels saturation and due to the plum impingement with the solar arrays [6], consecutive manoeuvres have to be separated by at least 48 minutes and their maximum allowed durations are  $\Delta t_{IPP,max} = 45$  s,  $\Delta t_{IPR,max} = 50$  s and  $\Delta t_{OOP,max} = 330$  s. Eventually, the manoeuvres should, on a best effort basis, avoid thruster firing during payload measurement.

### B. Characteristics of the optimisation algorithm

The described problem consists in multivariable and constrained optimisations, that are solved using a basic differential evolution method. The relations between the various cost functions are determined by their weights: the more important the cost function, the higher the value of its weight.

In the IP optimiser, with  $k_{\Delta l_0,max} = 20.0$  m $^{-1}$  and  $k_{e,max} = 10^7$ , the cost functions related to the mission constraints have the most significant contribution. Once these are satisfied, the required values are targeted with

$k_e = 10^6$  and  $k_{\Delta l_0} = 2.0$  m $^{-1}$ , whilst the times of the manoeuvres might be shifted having  $k_{SAR} = 10.0$  s $^{-1}$ . In this case the AoL of the manoeuvres are not controlled, so  $k_\alpha = 0.0$  deg $^{-1}$ . The maximum number of manoeuvres allowed per slot is set equal to  $n_{IP,max} = 3$ . Analogously, in the OOP optimiser the weights related to the constraints of the mission are the highest ( $k_{\Delta l,max} = 20.0$  m $^{-1}$  and  $k_{\Delta H} = 20.0$  s $^{-1}$ ). To achieve the desired results, the other weights are  $k_{SAR} = 10.0$  s $^{-1}$ ,  $k_{\Delta V} = 5.0$  m/s $^{-1}$ , and  $k_{\Delta t} = 0.05$  days $^{-1}$ .

The results are shown for two different examples. The first, starting on 2024-01-30, is a routine case, i.e. the initial point of the ground track is already within the boundaries. The second instead is a recovery case, starting on 2023-11-01. Both account for 60 days of propagation for the OOP computation, and 16 days for the IP.

### C. Routine case

*Analysed period: 2024.01.30 – 2024.03.23.*

The following example shows a routine case, i.e. the starting conditions of the ground track at the Equator and at maximum latitude are all nominal.

To maintain the evolution of  $\Delta l_0(t)$  within the limits for 16 days, two IP manoeuvres per slot are selected. In Tab. 1 the results for the first slot are reported, as well as the overall cost function for one ( $J_1$ ) and two manoeuvres ( $J_2$ ). The value of the latter proves that with two IP all constraints are met, and that the required ground track displacement and eccentricity are targeted efficiently. In Fig. 3, the evolution of  $\Delta l_0(t)$  is shown.

The requirements related to  $\Delta l_L(t)$  and  $\Delta H(t)$  are met with two OOP manoeuvres, which results are reported in Tab. 2. As for the IP, the requirements would not be met with  $n_{OOP} = 1$ , so two manoeuvres are selected (see Fig. 5).

*Tab. 1. Routine case IP manoeuvres, first slot.*

	Slot 1 – #1	Slot 1 – #2
$\Delta l_0$ [m]	54.442	228.279
$\Delta V$ [mm/s]	0.877	3.702
$\Delta t$ [s]	3.455	14.587
$\alpha$ [deg]	55.690	232.589
$t$ [MJD]	8799.007	8799.041
$t$ [UTC]	2024.02.03 @ 00:09:56	2024.02.03 @ 00:58:27
$J_1$ [-]	0.706787	
$J_2$ [-]	$3.493 \times 10^{-12}$	

Tab. 2. Routine case OOP manoeuvres.

	#1	#2
$\Delta L_L$ [m]	94.759	43.106
$\Delta V$ [mm/s]	111.523	50.732
$\Delta t$ [s]	320.221	145.670
$\alpha$ [deg]	359.963	0.033
$t$ [MJD]	8795.911	8823.856
$t$ [UTC]	2024.01.03 @ 21:51:15	2024.02.27 @ 22:56:43
$J_1$ [-]	21176512.763896	
$J_2$ [-]	8.929812	

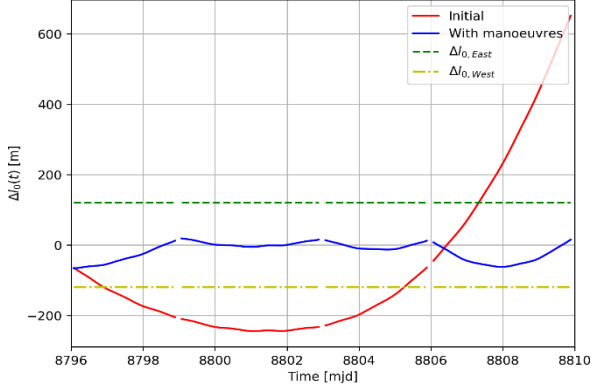


Fig. 3.  $\Delta l_0(t)$  before/after the manoeuvres, routine case.

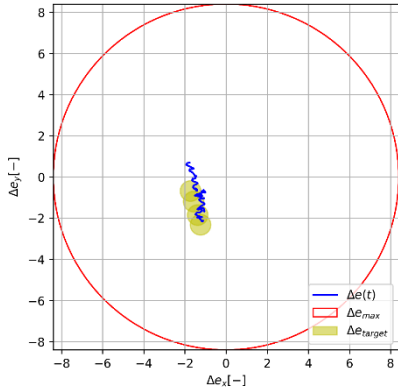


Fig. 4.  $\Delta e_y(t)$  vs  $\Delta e_x(t)$ , scaled of  $10^{-6}$ .

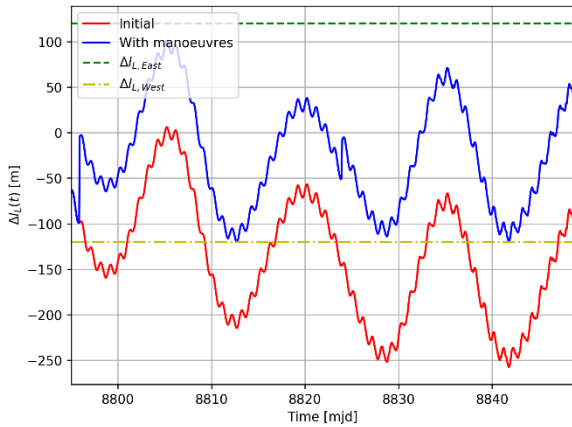


Fig. 5.  $\Delta L_L(t)$  before/after the manoeuvres, routine case.

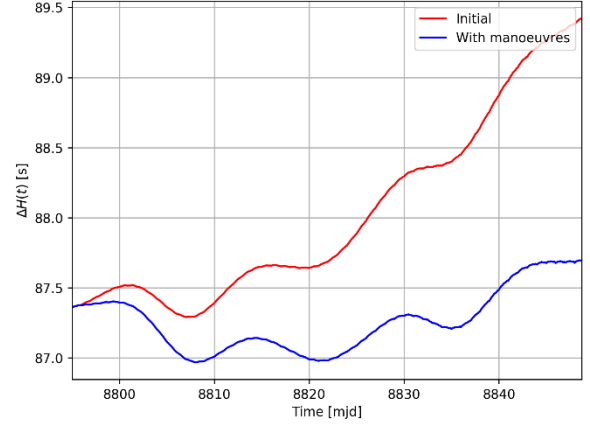


Fig. 6.  $\Delta H(t)$  before/after the manoeuvres, routine case.

#### D. Recovery case

Analysed period: 2023.11.01 – 2023.12.24.

As shown in Fig. 7, the initial point of the ground track at Equator in the recovery case is exceeding the boundaries. This example is presented to show how efficiently the algorithm brings the curve back into the limits. In Fig. 7, three slots of manoeuvres are presented, and the results of the first two are reported in Tab. 3 and Tab. 4. In the first slot, the cases of  $n_{IP} = 1, 3$  are discarded. The first does not allow to follow the structural requirements, and the later leads to an overall cost function that is worse than the two-manoevres case. Therefore, in this case, two full manoeuvres are needed to bring the ground track at Equator inside the limits as soon as possible. The second slot then follows with three manoeuvres, to target the required displacements  $\Delta l_{0,req}$  and  $\Delta e_{req}$ .

The ground track at maximum latitude, instead, meets the requirements with three manoeuvres. See Fig. 8 and Tab. 5 for the results.

Tab. 3. Recovery case IP manoeuvres, first slot.

	Slot 1 – #1	Slot 1 – #2
$\Delta l_0$ [m]	735.775	731.245
$\Delta V$ [mm/s]	11.490	11.490
$\Delta t$ [s]	45.0	45.0
$\alpha$ [deg]	109.422	286.210
$t$ [MJD]	8707.886	8707.919
$t$ [UTC]	2023.11.03 @ 21:15:27	2023.11.03 @ 22:03:57
$J_1$ [-]	Not possible	
$J_2$ [-]	66771153.309028	
$J_3$ [-]	66820559.910805	

Tab. 4. Recovery case IP manoeuvres, second slot.

	Slot 2 – #1	Slot 2 – #2	Slot 2 – #3
$\Delta l_0$ [m]	-740.975	430.081	316.0
$\Delta V$ [mm/s]	15.402	9.380	7.017
$\Delta t$ [s]	50.0	36.736	27.483
$\alpha$ [deg]	229.758	258.072	131.114
$t$ [MJD]	8711.886	8712.028	8712.073
$t$ [UTC]	2023.11.07 @ 21:15:30	2023.11.08 @ 00:40:46	2023.11.08 @ 01:44:41
$J_1$ [-]	365488.313188		
$J_2$ [-]	7067.999177		
$J_3$ [-]	23.573850		

Tab. 5. Recovery case OOP manoeuvres.

	#1	#2	#3
$\Delta l_L$ [m]	-84.356	-83.107	-7.161
$\Delta V$ [mm/s]	99.284	97.815	8.428
$\Delta t$ [s]	283.3	279.106	24.049
$\alpha$ [deg]	179.839	179.831	179.846
$t$ [MJD]	8711.945	8725.933	8746.916
$t$ [UTC]	2023.11.07 @ 22:40:33	2023.11.21 @ 22:23:52	2023.12.12 @ 21:58:33
$J_1$ [-]	85324290.999178		
$J_2$ [-]	2128.988559		
$J_3$ [-]	9.035304		

## VI. CONCLUSIONS

The algorithm outlined in this paper has demonstrated exceptional effectiveness in managing the orbit of the Sentinel-1A spacecraft, which operates within a low-Earth, sun-synchronous, frozen eccentricity orbit. Through careful selection of appropriate weight coefficients, the algorithm proves adaptable to various scenarios, including those arising from unexpected solar storms and the need for recovery following exceptional collision avoidance manoeuvres. In each instance, the method presented delivers a sequence of manoeuvres that uphold both orbital and mission constraints.

Moreover, the algorithm enables precise planning of out-of-plane manoeuvres, affording operators the ability

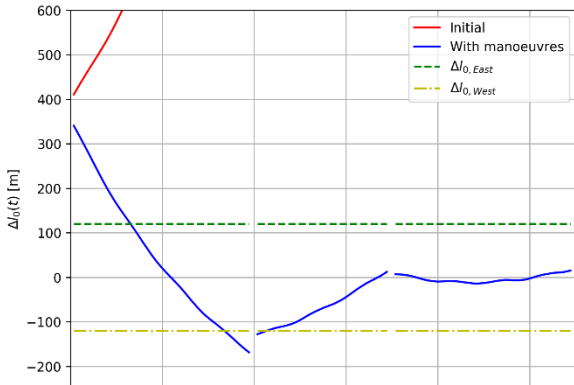


Fig. 8.  $\Delta l_0(t)$  before/after the manoeuvres, recovery case.

to anticipate such actions weeks in advance. Similarly, the prediction of in-plane manoeuvres adeptly addresses the unpredictability of solar activity. This capability significantly reduces the need for manual interventions by flight dynamics engineers, enhancing operational efficiency and reliability.

## VII. REFERENCES

- [1] Copernicus Programme official website, <<https://www.copernicus.eu/en>>, accessed March 2024.
- [2] M. Aorpimai, and P. L. Palmer, *Repeat-Groundtrack Orbit Acquisition and Maintenance for Earth-Observation Satellites*, Vol. 30, No. 3, Journal of Guidance, Control, and Dynamics, pp. 654-659, 2007, doi: 10.2514/1.23413
- [3] Xiaofeng Fu, Meiping Wu, and Yi Tang, *Design and Maintenance of Low-Earth Repeat-Groundtrack Successive-Coverage Orbits*, Vol. 35, No. 2, Journal of Guidance, Control, and Dynamics, pp. 686-691, 2012, doi: 10.2514/1.54780
- [4] P. Micheau, *Orbit control techniques for Low Earth Orbiting (LEO) satellites*, Spaceflight Dynamics Part I by Toulouse Space Center, edited by J. P. Carrou, Chapter 13, pp. 739-902, 1995
- [5] C. Valorge, J. C. Agnès, J. C. Bergès, J. L. Dulot, and J. Jaubert, *Processing orbit perturbations*, Spaceflight Dynamics Part I by Toulouse Space Center, edited by J. P. Carrou, Chapter 6, pp. 331-487, 1995
- [6] M. A. Martín Serrano, M. Catania, J. Sanchez, A. Vasconcelos, D. Kuijper, and X. Marc, *Sentinel-1A Flight Dynamics LEOP Operational Experience*, Proceedings 25<sup>th</sup> International Symposium on Space Flight Dynamics, 2015
- [7] J. Sánchez, M. A. Martín Serrano, and R. Mackenzie, *Characterization of the solar radiation pressure perturbation in the eccentricity vector*, 25<sup>th</sup> International Symposium on Space Flight Dynamics, 2015

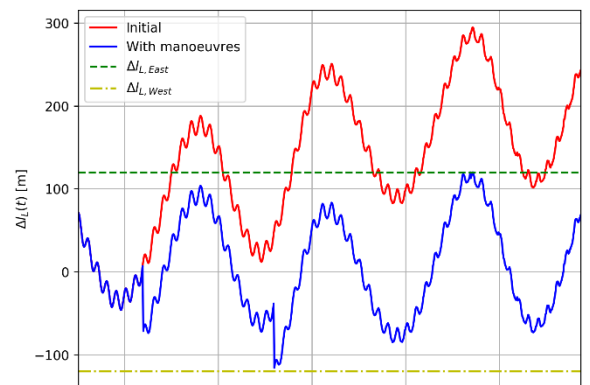


Fig. 7.  $\Delta l_L(t)$  before/after the manoeuvres, recovery case.